Earth Planets Space, **64**, 553–566, 2012

Equatorial F_2-layer variations: Comparison between F_2 peak parameters at Ouagadougou with the IRI-2007 model

O. S. Oyekola[1] and P. R. Fagundes[2]

[1]*307-143 Eighth Street, Etobicoke, Ontario, Canada M8V 3C8*
[2]*Universidade do Vale do Paraiba (UNIVAP), Sao Jose dos Campos, Sao Paulo, Brazil*

(Received June 17, 2011; Revised July 29, 2011; Accepted August 9, 2011; Online published July 27, 2012)

Observations of the F_2-layer critical frequency (f_oF_2), peak height F_2-layer (h_mF_2) and propagation factor ($M_{3000}F_2$) recorded near dip-equator Ouagadougou, Burkina Faso (12.4°N, 358.5°E; dip latitude: 1.5°N) have been validated against the International Reference Ionosphere (IRI-2007) model during low (1987) and high (1990) solar activity and undisturbed conditions for four different seasons, with a view to enhance the predictability of the IRI. The results illustrated that URSI option for h_mF_2 and CCIR option for $M_{3000}F_2$ portray remarkably well the morphological trends and replicate mostly the diurnal salient features of the experimental data at low and high solar activity periods. In contrast, both URSI and CCIR models of f_oF_2 also reproduce diurnal and seasonal patterns and outstanding features of observational data surprisingly well for solar minimum conditions except July; whereas we found considerable disparities between model and data during solar cycle maximum. The total model error ranging from approximately 6–8% (h_mF_2), 13–38% (f_oF_2) and 8–29% (h_mF_2), 12–44% (f_oF_2), respectively for low and high flux year, but roughly comparable at 3–7% for $M_{3000}F_2$ at low and high solar activity. Our observations indicate higher values of f_oF_2 deviations compared to prior calculated differences obtained for the low-latitude region over Indian and Asian.

Key words: Equatorial-ionosphere, F_2-layer, IRI-model, solar minimum-maximum.

1. Introduction

The International Reference Ionosphere (IRI) is the international standard for the specification of ionospheric densities, temperatures, and composition (e.g., Bilitza *et al*., 1979; Bilitza, 2001). The IRI (Bilitza, 2003) offers a valuable and evolving synoptic description of the average ionosphere, accounting well for the seasonal, spatial, and diurnal changes (Wilkinson, 2004). IRI has been used for a wide range of applications (e.g., Miller *et al*., 1990; Bilitza *et al*., 1995; Huang *et al*., 1996; Coetzee, 2004).

The F_2-region is the most important part of the ionosphere for propagation of high frequency (HF) signals. The key F_2-layer characteristics are the critical frequency (f_oF_2) and height of the F_2 peak electron density (h_mF_2). It is important to state that h_mF_2 values are not directly scaled from ionograms as are other ionospheric F_2-region parameters. As a result of group retardation of the radar wave, a practical approach to infer h_mF_2 values is to use empirical formulas that connect h_mF_2 to the maximum usable frequency (MUF) factor, $M_{3000}F_2$ parameter, rather than working with the virtual height read from the ionogram (Bradley and Dudeney, 1973). Thus, the derivation of the F_2 altitude using $M_{3000}F_2$ parameter requires use of semi-empirical models (Bradley and Dudeney, 1973; Bilitza *et al*., 1979).

$M_{3000}F_2$ is also a valuable ionospheric parameter defined as the ratio of the maximum usable frequency (MUF) at a distance of 3000 km to the F_2 layer critical frequency. $M_{3000}F_2$ is also called propagation factor. This parameter, in theory, represents the optimum frequency at which to broadcast a signal that is to be received at a distance of 3000 km (Oyekola, 2010). MUF can be routinely scaled from ionograms. International Radio Consultative Committee (CCIR) coefficients for $M_{3000}F_2$ have been obtained in the same way as for f_oF_2.

There are numerous reports on experimental discrepancies between IRI model predictions and ionosonde observations from different longitude sectors around the globe, for reviews see Obrou *et al*. (2003); Adeniyi *et al*. (2003); Sobral *et al*. (2003); Araujo-Pradere *et al*. (2004); Abdu *et al*. (2006); Zhang *et al*. (2004a, b); Bertoni *et al*. (2006); Lee and Reinisch (2006); Rios *et al*. (2007); Sethi *et al*. (2008); Yadav *et al*. (2010). However, except for the study by Bertoni *et al*. (2006), the quantitative areas of agreement and disagreement between model and data has not yet received much attention.

In this paper, we report a comparative analysis between IRI model-predicted ionospheric F_2-layer peak parameters from ionospheric observations obtained with an ionospheric sounder operated on a routine basis at a near equatorial station located at Ouagadougou (Burkina Faso: Geographic: 12.4°N, 358.5°E; dip latitude: 1.5°N). The disparities, which are observed to exist, will be helpful for advancement of the IRI model and of the CCIR numerical maps at sub-equatorial latitudes, mostly for the longitude sector

doi:10.5047/eps.2011.07.017

considered in this study, where ground-based observations are limited.

In the following sections, we first describe the base data used for this study together with information on the solar and geophysical conditions. We also highlight the "Bilitza" empirical formula used in calculating h_mF_2 (Section 2). In the observations section, a direct comparison between the observed and calculated ionospheric characteristics with their IRI model-predicted values is given in Subsection 3.1. A variation in the percent deviations of ionosonde-derived h_mF_2 and measured f_oF_2 and $M_{3000}F_2$ from their IRI model-predicted values is our focus in Subsection 3.2. This is followed by quantitative analyses of model performance (Subsection 3.3). Our results are discussed in Section 4. This paper is concluded with a summary of our key findings (Section 5).

2. Data Analysis

Ionosonde measurements were collected from Ouagadougou during 1987 low and 1990 high solar activity periods for low magnetic activity defined as K_p less or equal to 3. The yearly averaged smoothed sunspot numbers for the low and high solar activity periods were about 29, and 142.6, respectively. Four seasons were chosen: December solstice, March equinox, June solstice, and September equinox are represented by January, April, July, and October, in that order. Note that the inclusion of the two equinox seasons in our study rather than one will enable us to examine the differences between March and September equinoxes. The monthly averaged smoothed sunspot numbers, R_{12} for each of these months were 17.6 (January 1987), 24.4 (April 1987), 31.3 (July 1987), and 43.6 (October 1987) for the low solar activity period, whereas for the high solar activity period the corresponding mean values of the R_{12} were 150.6 (January 1990), 149.3 (April 1990), 140.6 (July 1990), and 142.1 (October 1990).

The f_oF_2 and $M_{3000}F_2$ data were from monthly tables of routinely scaled parameters for the station. The values of h_mF_2 were derived from "MUF factor" $M_{3000}F_2$ using the formula proposed by Bilitza *et al*. (1979). The "Bilitza formula", which allows for the effect of ionization below the F_2 layer, takes the form:

$$h_mF_2 \equiv \frac{1490}{M_{3000}F_2 + \Delta M} - 176 \text{ [km]}, \quad (1)$$

where

$$\Delta M \equiv \frac{F_1 * F_4}{(f_oF_2/f_oE) - F_2} + F_3, \quad (2)$$

with

$$F_1 \equiv 0.00232 * R_{12} + 0.222,$$
$$F_2 \equiv 1.2 - 0.016 * \exp(0.0239 * R_{12}),$$
$$F_3 \equiv 0.00064 * (R_{12} - 25),$$
$$F_4 \equiv 1 - R_{12}/150 * \exp(-\Phi^2/1600).$$

The correction term ΔM (Eq. (2)) thus includes the influence of underlying layers through the ratio f_oF_2/f_oE and the dependence on solar activity R_{12} (the averaged monthly smoothed value of sunspot number). f_oE is the critical frequency of E-layer, and Φ is the geomagnetic latitude of the location in question, for Ouagadougou, $\Phi = 15.4^\circ$N. The observed f_oF_2 and f_oE values were used in calculation of h_mF_2. Hourly monthly medians values were used for each case. F_2 peak height obtained this way is known as calculated h_mF_2.

Table 1. Percent normalized RMS errors for the altitude of the F_2 peak, F_2 critical frequency and propagation factor during 1987 low and 1990 high flux conditions[a].

Parameter	Season	Low flux	High flux
		Percent normalized RMS	
h_mF_2	Jan	8.3	8.2
	Apr	8.1	10.2
	Jul	7.3	28.8
	Oct	6.3	9.8
f_oF_2 (URSI)	Jan	15.7	12.1
	Apr	25.8	35.8
	Jul	31.9	34.2
	Oct	14.4	28.8
f_oF_2 (CCIR)	Jan	13.9	43.7
	Apr	32.2	39.4
	Jul	38.6	40.0
	Oct	16.1	31.1
$M_{(3000)}F_2$	Jan	3.0	3.2
	Apr	5.3	4.5
	Jul	5.1	7.3
	Oct	4.2	3.7

[a]Normalized RMS error is computed by taking the RMS of the data subtracted from the model results and then divided by the RMS of the data.

The IRI-2007 model values of h_mF_2, f_oF_2, and $M_{3000}F_2$ were downloaded from the IRI2007 website: http://nssdc.gsfc.gov/space/model/models/iri.html. The following IRI model options were considered for this study: IRI-URSI option for h_mF_2, IRI-URSI and IRI-CCIR options for f_oF_2, and IRI-CCIR maps for $M_{3000}F_2$.

The overall model error is estimated using normalized root-mean-square error for maximum height, maximum electron concentration, and propagation factor following the example of Pawlowski *et al*. (2008):

$$E = \frac{\sqrt{\langle (F_{\text{model}} - F_{\text{data}})^2 \rangle}}{\sqrt{\langle F_{\text{data}}^2 \rangle}}, \quad (3)$$

where E is normalized RMS error, the $\langle\rangle$ symbolizes taking a mean, F and observational data. At $E = 0$, the model and data agree perfectly, while at $E = 1$, the model could be replaced by a zero line. With the value of $E > 1$, the model results are diverging from the data, and most likely the model does not trend the data. The results are set out in Table 1, as we shall see later.

3. Results

In this section, we present in detail the morphological patterns between global model and ionosonde observations for low and high solar activity periods during the solstices, vernal, and autumnal seasons. A percent deviation of ionospheric experimental observations from model predictions is discussed. In contrast to the visual evaluation of the model, the detailed quantitative comparisons, which are

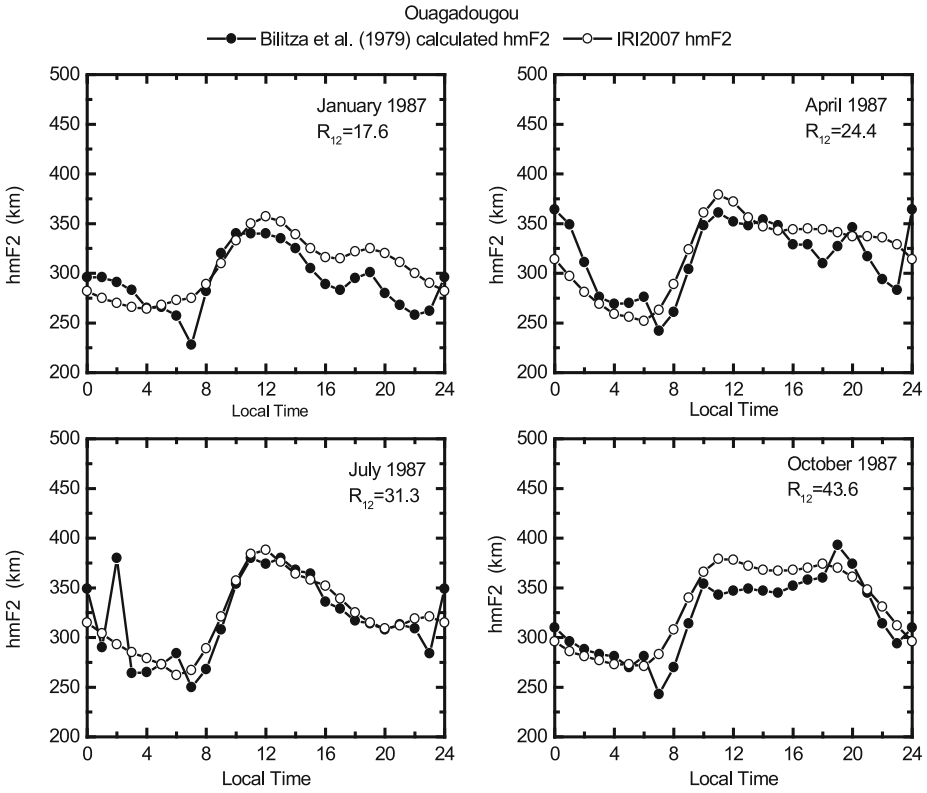

Fig. 1. Diurnal and seasonal variations of monthly median values of h_mF_2, compared with the IRI-2007 predictions at Ouagadougou during solar cycle minimum of 1987.

necessary for application purposes will be addressed in this section also.

3.1 Comparisons of ionosonde-inferred h_mF_2, measured f_oF_2 and $M_{3000}F_2$ and IRI model predictions for Ouagadougou

A direct comparison is made between calculated h_mF_2, measured f_oF_2 and $M_{3000}F_2$ with model predictions for four different seasons during solar cycle minimum and maximum for quiet-time in Figs. 1–6. The 12-month running mean value of the sunspot number for each month is shown in each panel. Each figure contains four panels of plots representing the month of January (left top), April (right top), July (bottom left), and October (bottom right). In order to aid comparison, observed and predicted values of F_2-region peak parameters are plotted together for four different seasons in Figs. 1–6.

Figure 1 displays the comparisons between calculated and IRI model-predicted h_mF_2 values during low solar flux for four seasonal periods. As can be seen, the figure indicates a rough uniform behavior of h_mF_2 for the four seasons, with early morning minima, pre-noon, post-dusk peaks, respectively. There is also an apparent midnight measured peak, in all months, even though it is small in October. Post-dusk peaks are not apparent in equinoxes, but very small peaks are obvious during December solstice in IRI representation of h_mF_2. Post-sunset maximum are completely absent for both model and estimated h_mF_2 during the month of July. Postsunset h_mF_2 enhancements are much intensified during equinoxes for calculated h_mF_2. One may also note that the discrepancy between model and calculated h_mF_2 seems to be larger between about local midday and 2300 LT in January. In general, IRI slightly overestimates the calculated h_mF_2 for all seasons, except for month of July, where the model nearly matches with the observed data for the periods 0800–2200 LT.

Figure 2 compares "Bilitza" h_mF_2 with those of IRI values during high solar flux conditions of the year 1990. It is clear from Fig. 2 that the modeled h_mF_2 follow the behavior of the estimated data for each season. The striking features in the diurnal cycle given in Fig. 2 are near sunrise minima and a sharp increase during daytime to reach well-defined post-sunset maxima at about 2000 LT for all seasons for calculated h_mF_2 data. It is interesting to see that IRI-URSI 2007 model does replicate the postsunset peaks in h_mF_2 and indeed it is precisely at those peaks where experimental and modeled curves coincide except July. The fact that IRI peaks look smooth as compared with those measured is ought to overestimations at previous local times before the occurrence of postdusk peaks. In addition, post-midnight maximum is evident only in April. There is also a good fit between the calculated h_mF_2 and IRI curves during post-midnight sector. Here the model results largely overestimate the calculated h_mF_2 during the daytime, except for the month of July, where disparities are somewhat large around postsunset hours.

In Fig. 3, diurnal and seasonal cycles of measured and modeled f_oF_2 values are presented for 1987 low solar minimum conditions. Apparently, both the URSI and CCIR options follow the experimental f_oF_2 curves in January and October. Experimental f_oF_2 is lower in value between 1100 and 1500 LT in January. During April and July, the model grossly underrepresents the critical frequency val-

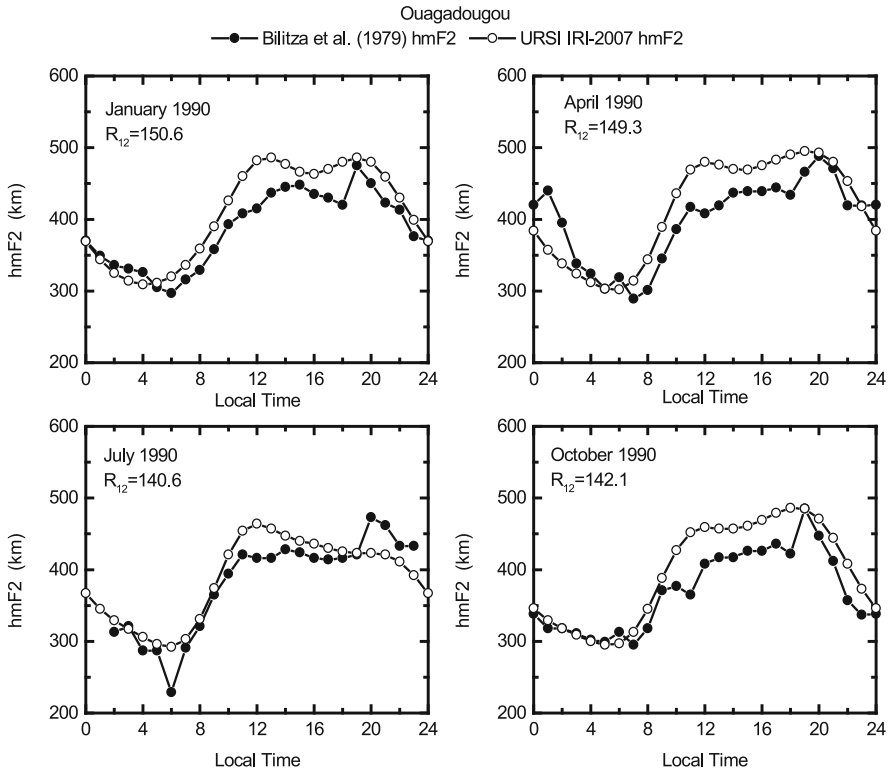

Fig. 2. Results similar to those of Fig. 1, but for the solar activity maximum year 1990.

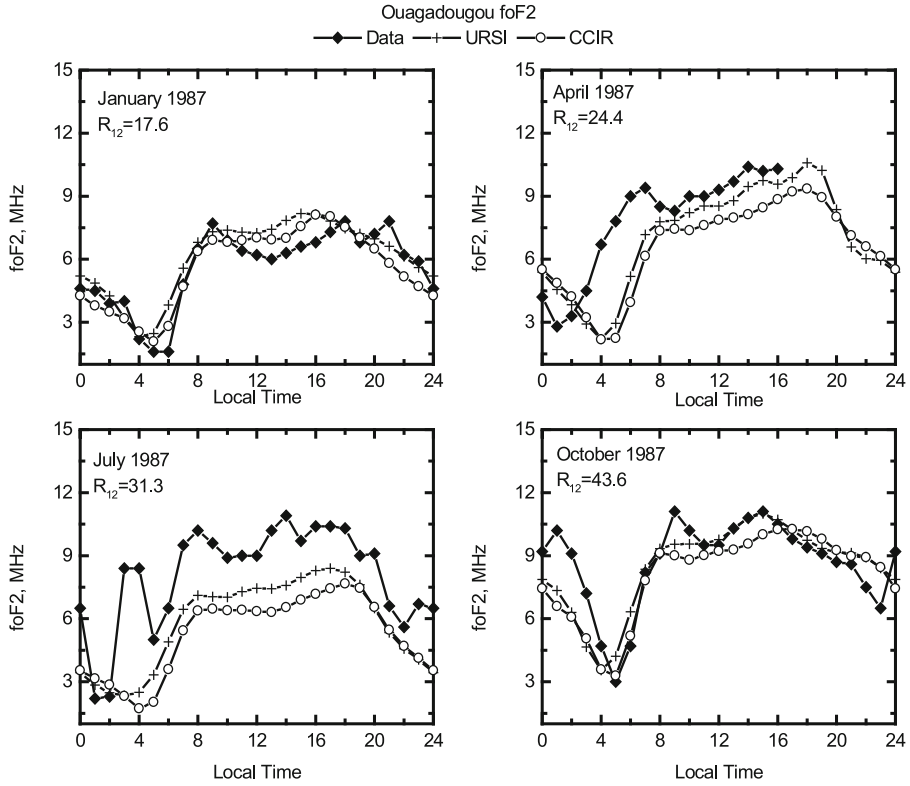

Fig. 3. Diurnal and seasonal variations of monthly median values of f_oF_2, compared with the IRI-2007 predictions at Ouagadougou during solar cycle minimum of 1987.

ues. Notice that in April, we do not have complete data. The data exist between 0000 and 1600 LT. However in July, ionosonde measurements indicate substantial fluctuations with several peaks with magnitude consistently and radically than the IRI ones. Both IRI curves behave as a minimum baseline from about 0300–2300 LT in July, but from about 0300–1600 LT in April. In October, the measured f_oF_2 is higher than the modeled values between local

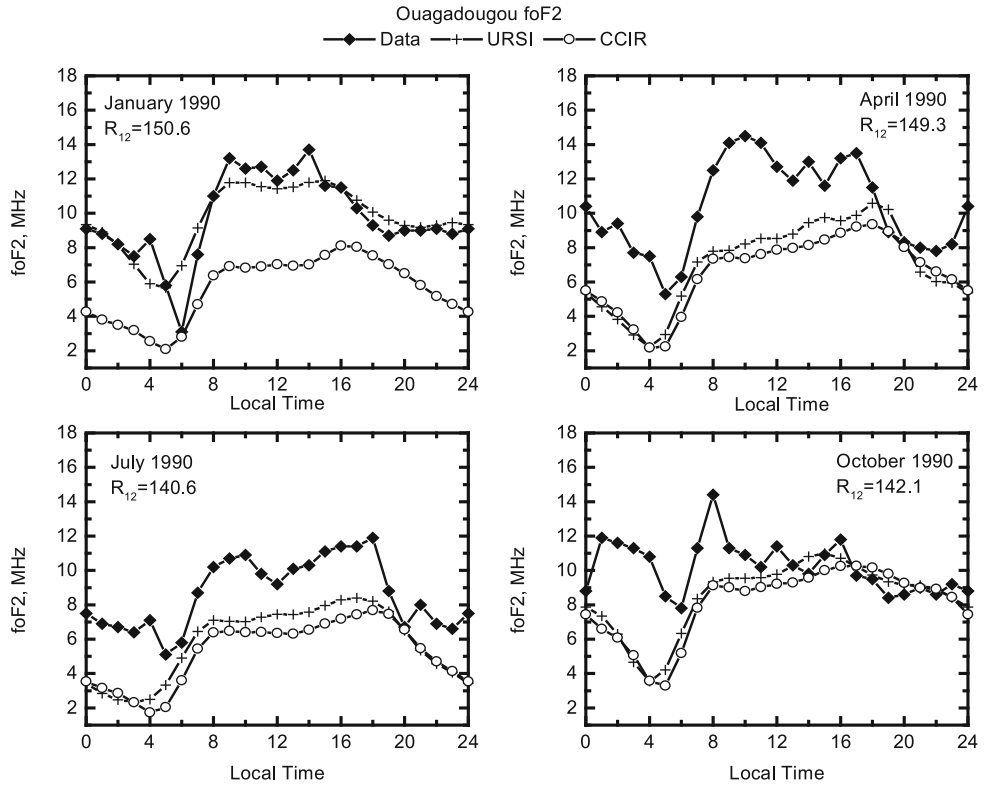

Fig. 4. Results similar to those of Fig. 3, but for the solar activity maximum year 1990.

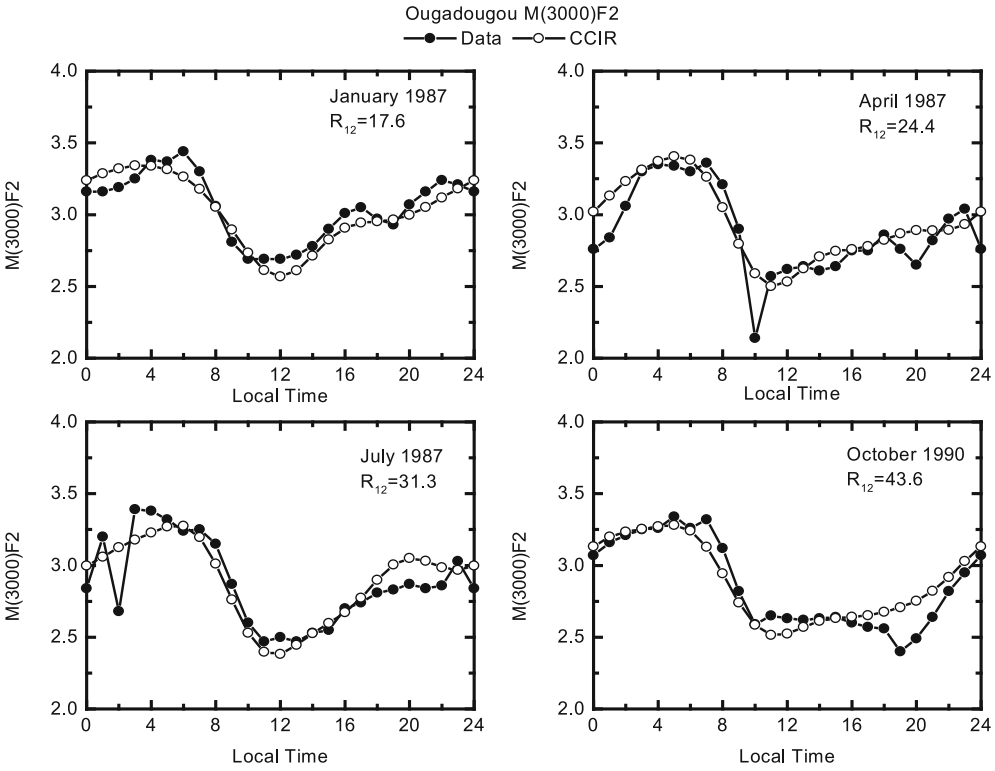

Fig. 5. Diurnal and seasonal variations of monthly median values of $M_{3000}F_2$, compared with the IRI-2007 predictions at Ouagadougou during solar cycle minimum of 1987.

midnight and 0500 LT. Notice that October curves indicate deep minima for both ionosonde and the IRI model. These minima occur at about 0300 LT in IRI and roughly 1-hour later for ionosonde. One other interesting feature found in the ionosonde data is the near local noon minimum (midday "bite-out"), which occurs in all seasons. This feature is not well formed by the simulated curves. Our results generally show that f_oF_2 parameter is disgustingly underrep-

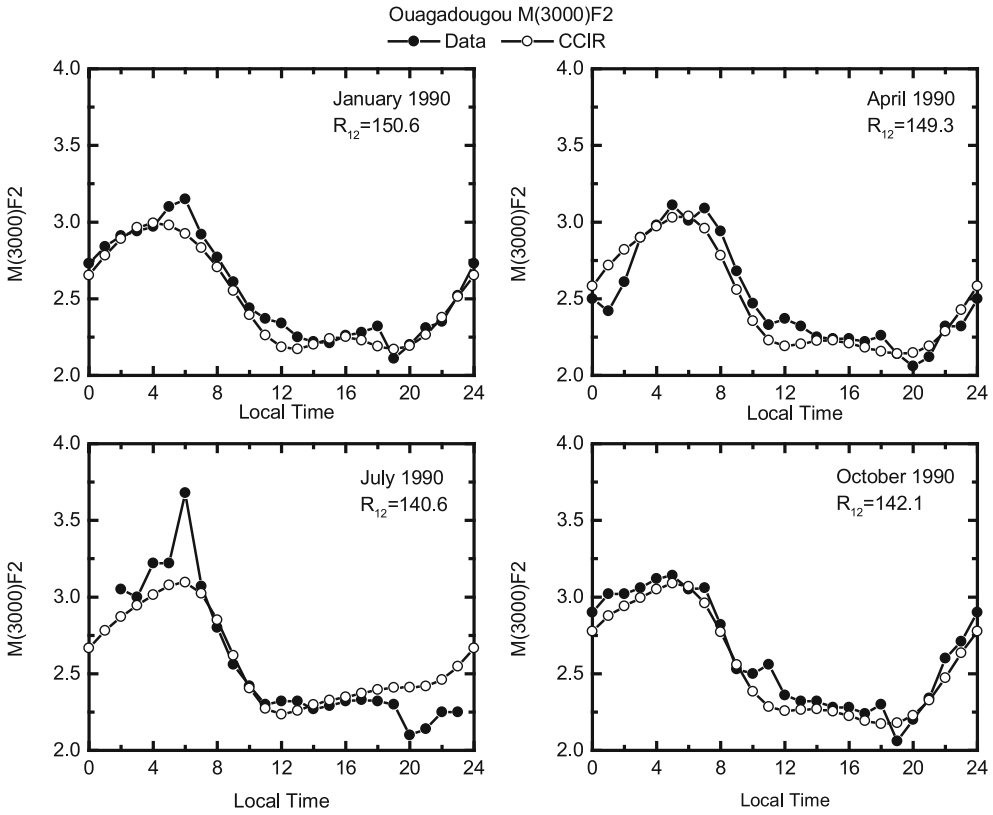

Fig. 6. Results similar to those of Fig. 5, but for the solar activity maximum year 1990.

resented by both URSI and CCIR options for f_oF_2 during the daytime and nighttime periods. This result is consistent with Bertoni *et al.* (2006) who found f_oF_2 to be underestimated for the station Palmas (10.17°S, 48.20°W, dip: −10.80°) during low solar activity period of 2003–2004.

Figure 4 compares the observed monthly median f_oF_2 and IRI model results for four seasonal periods during high solar flux and magnetically quiet times. In January IRI-URSI f_oF_2 provides a better fit, except for the periods 0800–1600 and 1800–2000 LT. The three curves agree between about 1800 and 2000 LT in April. During the month of July, IRI-URSI prediction curve is closer to the ionosonde curve between 0400 and 0600 LT and again between 1900 and 2000 LT. In October, URSI and CCIR f_oF_2 values and the observed data are in reasonable agreement between about 1100 LT and local midnight. A careful inspection of Fig. 4 reveals the following outstanding characteristic features of the diurnal variation of f_oF_2, e.g., the appearance of sunrise or early morning minimum, the forenoon, postnoon and evening ionization maxima, midday "bite-out", as well as postsunset and postmidnight peaks of f_oF_2. These characteristic features are much more pronounced at high solar activity than at low solar activity. Some features are not distinct in the model; some are not reproduced by the IRI. For instance, post-midnight peaks are not noticed in model curves for all seasons. Also, early morning minimum of f_oF_2 does not occurs at the same time, the occurrence time differs by about 1–2 hours with model diurnal cycle minimum appears earlier for all seasons. Generally, poor agreement is obtained for F_2-layer critical frequency during high solar activity. Our results contrast the report of Batista and Abdu (2004) who found good agreement between the IRI predictions and observed mean f_oF_2 for the Brazilian equatorial station of Sao Luis (2.3°S, 44.2°W; dip angle: −2.7°) during high solar activity period.

Figure 5 shows the measured and modeled $M_{3000}F_2$ values for low solar activity for four different seasons. As can be seen the overall diurnal cycle of $M_{3000}F_2$ is well represented by the CCIR model, but some vital features such as the minimum at 1000 LT (April), 0200 LT (July), and 1900 LT (October) are not portrayed by the model curves. A direct comparison between the observed and IRI-CCIR predicted values of propagation factor during a period of high solar activity are given in Fig. 6 for four seasonal periods. We find a remarkable agreement between $M_{3000}F_2$ and the CCIR maps, apart from observed peaks seen in the experimental curves at about 0600 LT (January), midday (April), 0700 LT (July), and 1100 LT (October). July model curve does not indicate the dawn maximum and postsunset minimum clearly demonstrated by the ionosonde curve. Our data (observations 5 and 6) are in good agreement with the work of Obrou *et al.* (2003) but disagree to a large extent with the results given by Adeniyi *et al.* (2003), even for the same African longitude sector.

3.2 Variations in the percent deviations of ionosonde-derived h_mF_2, measured f_oF_2, and $M_{3000}F_2$ from IRI model predictions

In this subsection, we now examine the deviations of measured and calculated characteristics of the F_2 region with the expected values from the IRI model in an attempt to have a critical view of the reliability of the IRI predictions

over the equatorial region in the African sector. Therefore, the hourly percent deviation, $\%dX$ of each of the examined ionospheric parameter is computed using the expression:

$$\%dX = \frac{[X(\text{IRI}) - X(\text{calculated/measured})]}{X(\text{calculated/measured})} \times 100, \quad (4)$$

with X the hourly monthly-median values of each parameter (measured: f_oF_2 and $M_{3000}F_2$, calculated: h_mF_2).

Figure 7(a) shows the percent deviations between the IRI-URSI model results and the calculated values of the F-region peak height, h_mF_2 as a function of time of day and season for low sunspot period for Ouagadougou according to Eq. (3). Obviously, there is a trend of positive difference, implying that the model overestimates h_mF_2 values between 0500 and 2200 LT (January), 0700–1300 LT, 1600–1900, 2100–2300 LT (April), in most of the hours in July and from 0700 and 1800 LT (October). The deviation dh_mF_2 is as high as ∼20% in January and as low as ∼25% in July. Seasonal differences are observed for all local time, where the percent absolute deviations are largest (∼0–22.9%) for July and smallest (1.4–16.1%) for April, with a medium value of 0.8–16.4% and 0.2–20.8% for October and January, respectively. The seasonal averaged absolute deviation is from a near zero value to 19% during low solar activity period.

Figure 7(b) presents the diurnal and seasonal cycles of the percent deviations between IRI-URSI h_mF_2 and calculated h_mF_2 for high solar flux and quiet geomagnetic activity conditions for Ouagadougou. Again, it is quite obvious that IRI model consistently overestimates ionosonde curves shown in Fig. 2, apart from local midnight to 0400 LT (January), 0000–0600 LT (April), 2000–2300 LT (July), and 0400–0600 LT (October) time intervals. We note that the model drastically overpredicts ionosonde-derived h_mF_2 by about 30% during sunrise hour in the month of July. The trend in the percent deviation clearly varies with season. The strongest effects are seen in July, 0–27.6%, and October, 0–23.8%, while the variations in January and April are not as large. The smallest variations are seen in January: 0.2–16%, with a medium value of 0–19% in April. Overall, the deviation ranges from 0–22%. Thus, the disparities between calculated h_mF_2 and IRI model-predicted h_mF_2 values during high solar activity are found to be insignificantly smaller (∼3%) than those differences observed for low solar activity period.

Figure 8(a) displays the typical characteristics of the diurnal and seasonal percent deviations between IRI-URSI f_oF_2 (solid circle) and IRI-CCIR f_oF_2 (open circle) and observed f_oF_2 during low solar activity year of 1987 under quiet magnetic activity conditions. We do not have observational data for April 1987 for the periods 1700–2300 LT, so there is no comparison within these local time intervals. The percent relative deviation is dominated by negative trend in April and July, implying that the measured values of f_oF_2 are constantly higher than the modeled f_oF_2 values (see observation 3). The model overestimates the measured value from 0400–0700 LT and 1100–1600 LT (January), 0000–0200 LT (April), 0100–0200 LT (July), and 0500–0600 LT (October). The modeled F_2-layer critical frequencies closely follow the behavior of the data during October month from 1100 and 2100 LT. We also note that the percent deviation curves indicate a sharp increase of about ∼75% (CCIR) and ∼140% (URSI) at dawn in January, ∼60% (URSI) and ∼70% (CCIR) at 0100 LT in April, ∼30% (URSI) and ∼40% (CCIR) at 0100 LT in July, and ∼40% for URSI at 0500 LT in October. CCIR shows no such increase in October. Furthermore, the trend in the IRI-URSI percent absolute deviation indicates strong and broad range of seasonal disparity. The largest effect is typically observed in January (∼1.2–138.7%) and smallest occurred in October (0–40%), with April (4.5–67%) and July (7.7–72%) lying between the two extremes. On the contrary, IRI-CCIR largest seasonal dissimilarity is found in July (16–79%), January (0–76%), and April (10–74%), with the lowest value found in October (0–35%). In general, the percent deviation of about ∼3–80% (URSI) and ∼7–66% (CCIR) are found for 1987 low solar activity year.

Figure 8(b) gives the local time and seasonal variations of percent deviations between IRI-URSI f_oF_2 (solid circle) and IRI-CCIR f_oF_2 (open circle) and the measured f_oF_2 during solar maximum of 1990 for low magnetic activity. Figure 8(b) indicates clearly that both IRI options for critical frequency of F_2-layer appear to be less accurate for equatorial region in Africa. Again, in January the deviation curve shows a relatively sharp increase in f_oF_2 with typical value near 125% for URSI model, indicating that IRI-URSI option overpredicts f_oF_2 data by that significant amount at sunrise. The URSI model percent deviation, df_oF_2 shows strong seasonal changes with largest value found in December solstice (0–124%), and lowest value occurred in June solstice (3–65%) with equinoxes (April: 0–70%, October: 0–67%) lying between the solstices extreme, whereas CCIR model indicates largest value in June solstice (July: 2–76%), December solstice (January: 9–70%), and March equinox (April: 0–71%), with the smallest value seen in September equinox (October: 0–67%). On average, absolute deviation of modeled f_oF_2 from observational data ranging from 0–80% and ∼3–70% for URSI and CCIR model, respectively for 1990 high solar activity year. Putting Figs. 8(a) and 8(b) together, we infer that overall deviations during solar minimum and maximum years are comparable for URSI option, but are marginally difference for CCIR model.

Figures 9(a) and 9(b) present the diurnal variations of percent discrepancies between the measured $M_{3000}F_2$ and the IRI-CCIR model-predicted $M_{3000}F_2$ for four seasonal phases in 1987 (Fig. 9(a)) solar minimum and 1990 (Fig. 9(b)) solar maximum year, in that order. As can be seen, there exist marked seasonal differences for the two levels of solar phases. During low solar activity, we found that the model overpredicts the measured value considerably by ∼21% in April at 1000 LT, ∼17% in July at 0200 LT, and ∼13% in October at 1900 LT. Here the deviation ranges from 0–14% over the four seasonal periods. At high solar activity year, Fig. 9(b), the morphological patterns of percent deviations exhibit positive and negative trends. The variation is obviously erratic. The changes indicate a relatively sharp increase of about 12% in April at 0100 LT, ∼15% in July at 2000 LT, and a deep minimum of ∼16% at sunrise also in the month of July. Here, the mean absolute deviation is between ∼0–12 percent. We observe that the changes in percent deviation during high solar activity

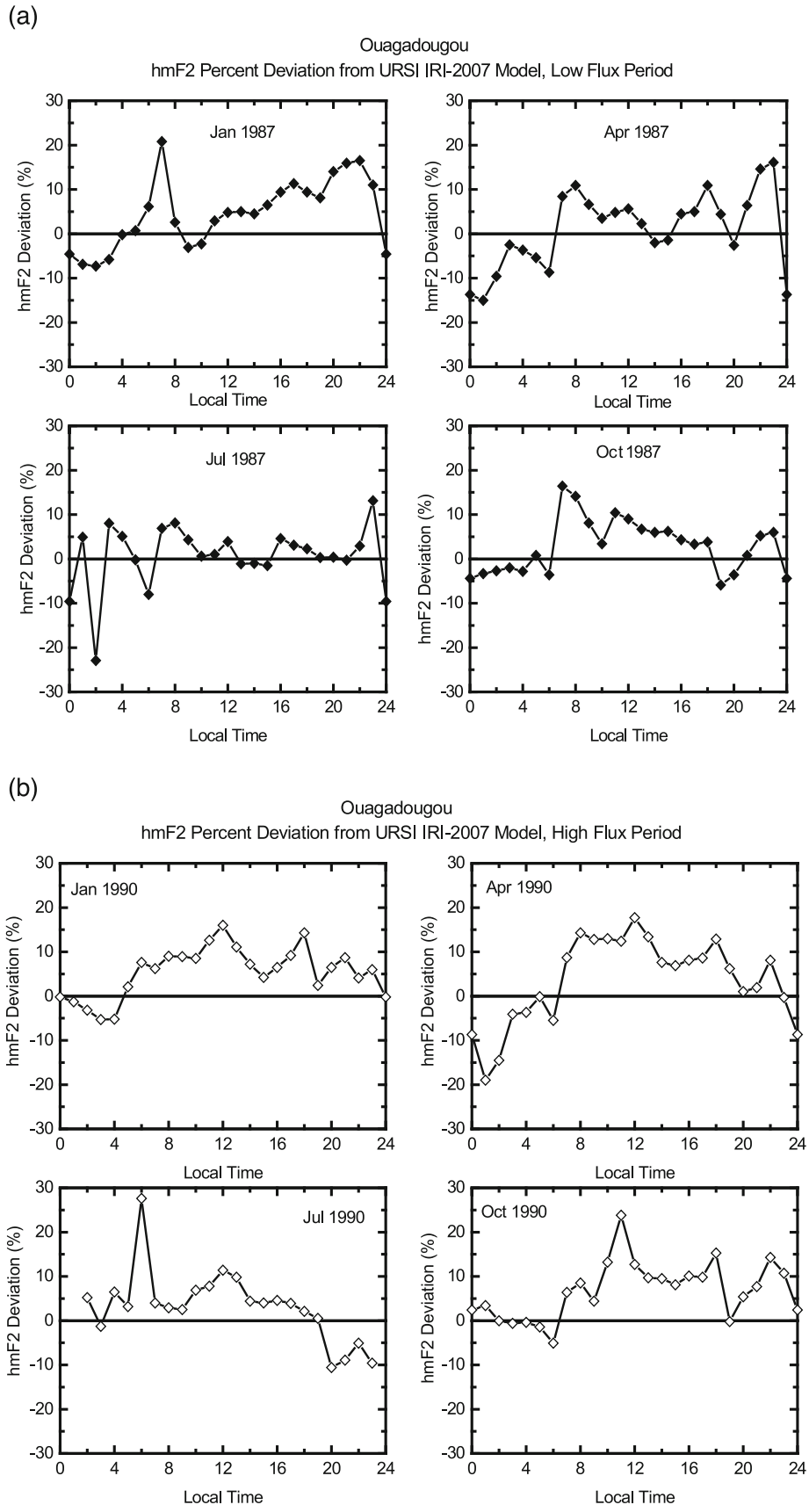

Fig. 7. (a) Local time and seasonal variations of percent deviations of calculated h_mF_2 from IRI predictions over Ouagadougou during low solar flux period of 1987. (b) Results similar to those of Fig. 7(a), but for the solar activity maximum year 1990.

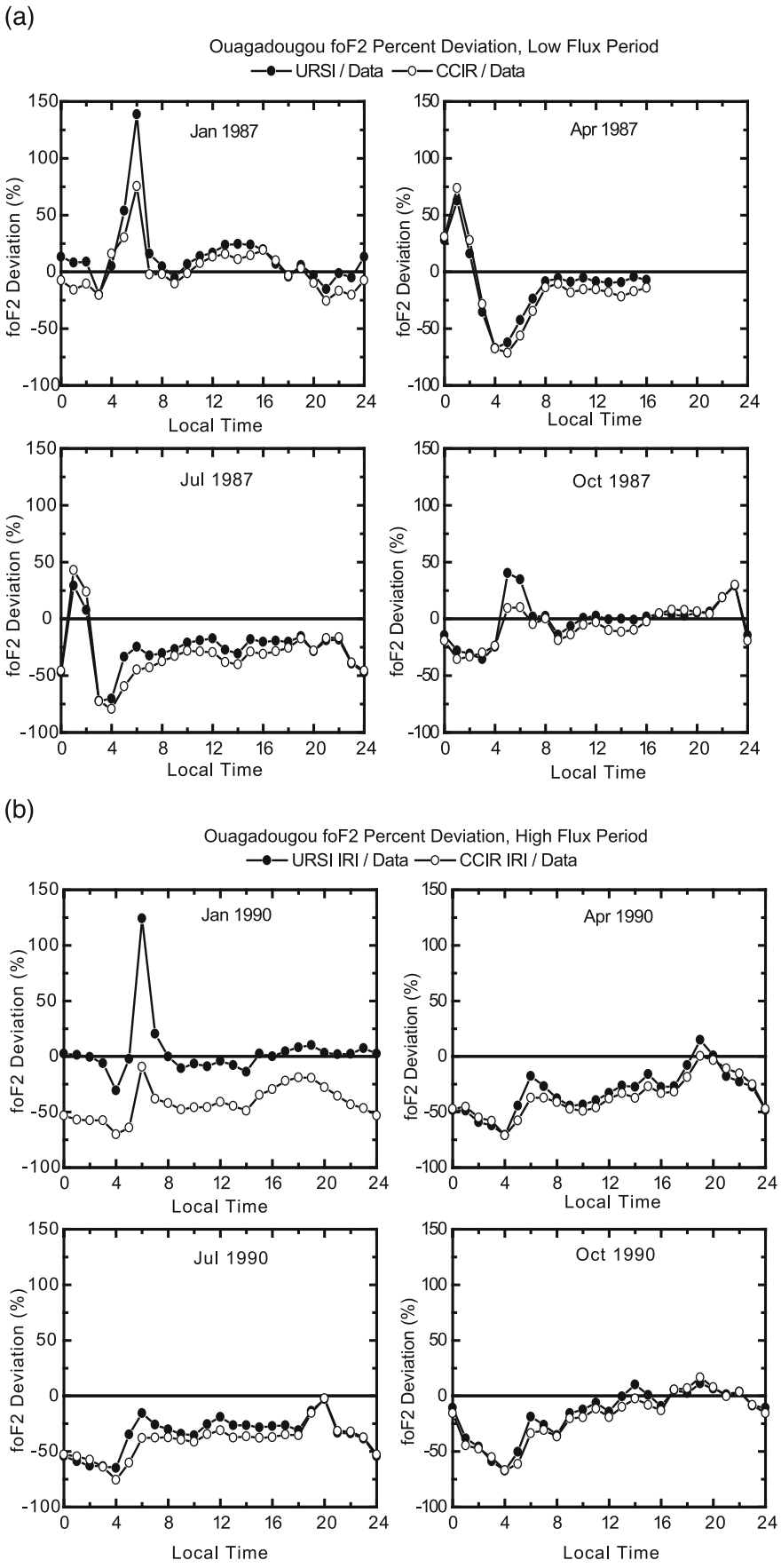

Fig. 8. (a) Local time and seasonal variations of percent deviations of measured f_oF_2 from IRI predictions over Ouagadougou during low solar flux period of 1987. Solid circle: IRI URSI model. Open circle: IRI CCIR model. (b) Results similar to those of Fig. 8(a), but for the solar activity maximum year 1990.

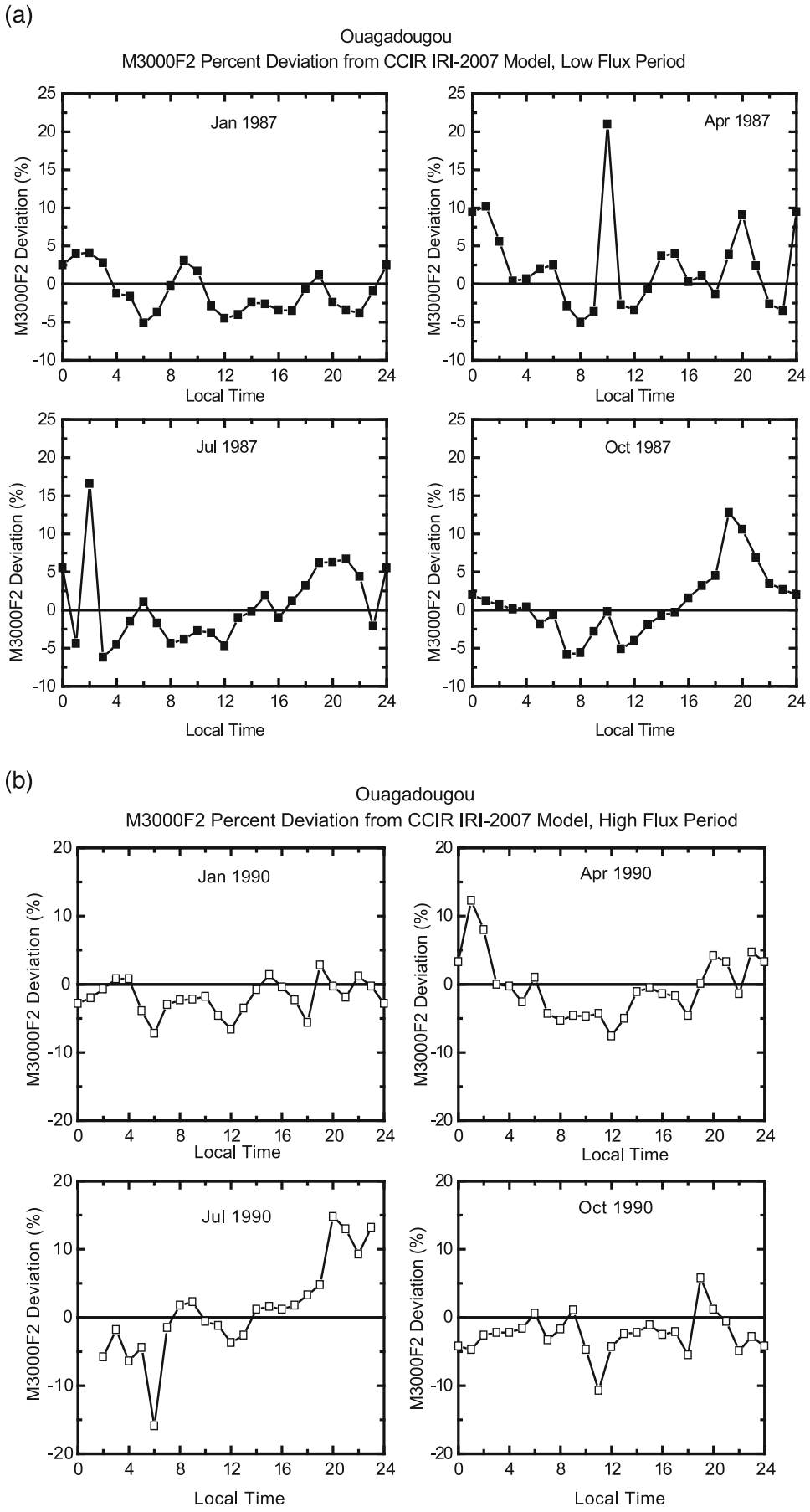

Fig. 9. (a) Local time and seasonal variations of percent deviations of measured $M_{3000}F_2$ from IRI predictions over Ouagadougou during low solar flux period of 1987. (b) Results similar to those of Fig. 9(a), but for the solar activity maximum year 1990.

is about 2% less than the variations seen during low solar activity year of 1987. In addition, the morphological patterns and trends of percent deviations, $dM_{3000}F_2$ shown in Figs. 9(a)–9(b) indicate striking seasonal differences. The range of variation is characteristically 0–5% (January), 0–21% (April), 0–17% (July), and 0–13% (October) for low sunspot period, while those of high sunspot year ranging from 0–7%, 0–12%, 0–16%, and 0–11% in January, April, July, and October, respectively.

The results of comparative analysis for h_mF_2 and f_oF_2 presented above agree qualitatively and contrast quantitatively the recent observations obtained for low-latitude regions in the Indian and Southeast Asian longitude sectors. Chuo and Lee (2008) used observed f_oF_2 and h_mF_2 made from the northern crest of equatorial ionization anomaly (EIA) station, Chung-Li (Taiwan: 24.9°N, 121.1°E; dip 35°) and compared with IRI-2001 model predictions for the period from 1994 to 1999. They showed that the percentage deviation of the observed f_oF_2 (h_mF_2) values with respect to the IRI model varies from 5–80% (0–25%) during nighttime and 2–17% (0–20%) at daytime, respectively. Sethi *et al.* (2008) used measured h_mF_2 derived from digital ionosonde measurements at a low to middle latitude station, New Delhi (India: 28.6°N, 77.2°E; dip 42.4°N) for the period from January 2003 to December 2003 and January 2004 to December 2005, reported that the percentage deviation of the observed h_mF_2 values with respect to the IRI-2001 model, in general, remains within 15% and 10% in all seasons during moderate and low solar activity, respectively. The deviations found in the present analysis are generally much greater than the deviations reported by Sethi *et al.* (2008). Yadav *et al.* (2010) used observed f_oF_2 and h_mF_2, and calculated h_mF_2 from modern digital ionosonde observations, again at EIA region, Bhopal (India: 23.2°N, 77.6°E; dip 18.5°N) during solar minimum year of 2007. The authors indicated that ionosonde measured h_mF_2 values show a good agreement with the calculated h_mF_2 values. They found IRI to exhibit a better agreement for h_mF_2 than for f_oF_2. Also, they pointed out that the percent difference between the model and observations remains less than 25% for all seasons, while percentage deviations for both measured and "Bilitza" calculated h_mF_2 values are less than 15%, in partial agreement with our observations.

3.3 Quantitative analysis

To quantitatively describe the visual agreement between the IRI model-predicted results and our ionosonde observations, we conducted normalized root mean square (RMS) error according to Eq. (3). The results are shown in Table 1. We can see that the normalized RMS error varies with season and the phases of solar cycle. The normalized RMS for altitude of the F_2 peak is from 6.3–8.3% (low solar activity year) and 8.2–28.8% (high solar activity year). We note that the error during high solar flux June solstice periods is exaggerated compared to low solar activity value, where there is a difference of nearly a factor of 4. Also shown in Table 1 are the errors in the critical frequency of F_2-layer for both URSI and CCIR options. For IRI-URSI f_oF_2, the differences between the errors for the ranges of solar flux values are not much, except for the month of October, where the high solar flux error doubled the low flux error. On the other hand, for CCIR f_oF_2, error in f_oF_2 during January and October high solar activity is a factor of 3 and 2 higher than those errors found in f_oF_2 during similar months of low solar activity, respectively. The normalized RMS errors for propagation factor show no significant changes to solar variability.

Table 2. The percent standard relative deviation of data from their respective medians for F_2 peak altitude, F_2 critical frequency, and propagation factor for 1987 low and 1990 high solar activity conditions.

Parameter	Season	1987 low flux	1990 high flux
		Percent relative deviation	
h_mF_2	Jan	8.1	11.6
	Apr	9.6	10.7
	Jul	11.1	12.1
	Oct	10.4	13.3
f_oF_2	Jan	23.2	21.1
	Apr	20.4	23.7
	Jul	19.5	20.5
	Oct	16.6	12.1
$M_{(3000)}F_2$	Jan	6.3	11.6
	Apr	8.7	11.0
	Jul	8.7	13.7
	Oct	10.1	12.3

Hence, quantitatively, there exist good agreement between CCIR model and the measured $M_{3000}F_2$ values with a fluctuations level of about 5% for both level of solar activity. The agreement between modeled and calculated h_mF_2 is also good with overall model error of less than 10% during low solar activity year of 1987. At high solar activity, model error is within approximately 8–10%, except for the month of July which is ∼29%, implying the agreement is comparatively good. As expected, the averaged normalized RMS errors for f_oF_2 are from 22–39%, which indicates poor agreement between observed and expected value of f_oF_2.

We further examine the percent standard relative deviations of the data from their respective medians. The results are given in Table 2 for both low and high solar activity periods. Interestingly, we found no substantial change between seasonal and solar cycle variations of the percent relative deviation for all the parameters. Taking Tables 1 and 2 together, for example, h_mF_2 value in January, for low solar activity year, the overall model error is estimated at 8.3%, whereas the relative deviation of h_mF_2 from the median is found to be 8.1%. So the model error is 0.2% less than the data scatter around median.

It is interesting, however, to contrast F_2-layer critical frequency analysis results obtained from the present study with the recent results presented by Oyekola (2011) within West-African sector, Ouagadougou, Burkina Faso (12°N, 1.5°W; dip latitude: 1.5°N) and Ibadan, Nigeria (7.4°N, 3.9°E; dip latitude: 2.3°S). Using observational data collected from Ibadan during very high solar activity year of 1958, yearly-averaged sunspot number $R_{12} = 184.8$ for quiet geomagnetic conditions. CCIR model of f_oF_2 was chosen. The hourly percent deviation ($\%\Delta f_oF_2$) varies from −11% to 12% (March), −34% to 11% (June), −16% to 12% (September) and −10% to 13% (December). The

model error ranges between about 50–125% over the four selected months, with maximum error occurring in the month of June. On the other hand, the present analysis utilizes ionosonde data acquired from Ouagadougou during high solar activity year of 1990, yearly mean sunspot number $R_{12} = 142.6$ for quiet-day F_2-layer. Both URSI and CCIR models of f_oF_2 were used for the study. The hourly percent deviation is as follows: January: -30% to 124% (URSI) and -70% to -9% (CCIR), April: -70% to 15% (URSI) and -70% to near zero % (CCIR), July: -65% to -3% (URSI) and -76% to -2% (CCIR) and October: -67% to 11% (URSI) and -67% to 17% (CCIR). Here, the total normalized root mean squared difference is typically within approximately 12% to 35% (URSI) and 30% to 44% (CCIR). On the basis of these results, the following main points are in order: (1) CCIR f_oF_2 model consistently presents substantial hour-to-hour and season-to-season percent deviation over Ouagadougou compared to that of Ibadan, while Ibadan demonstrates higher values and wider range of model error than those of Ouagadougou for similar undisturbed geomagnetic conditions but appreciably different yearly-averaged sunspot number, ∼23% difference in R_{12} values. (2) The substantial disparity in value of Δf_oF_2 is partly probably due to peculiarity in magnetic hemisphere, even though the stations are almost close to dip magnetic equator. (3) F_2-layer critical frequency results in such a narrow longitudinal range represent the complicated behaviors of the f_oF_2 parameter derived from equatorial ionograms and hence equatorial ionosphere.

4. Discussion

The current research pays so much attention to see how far the quiet-day ionosonde-inferred equatorial F_2-layer characteristics parameters compare with their IRI representations for eventual improvement of IRI forecasting capability. Almost all previous studies have typically focused on the F_2 peak characteristics provided by ionosondes, in particular critical frequency of F_2 layer and F_2 maximum height of electron density seem to be heavily compared with the IRI model compared to other ionospheric parameters such as ionospheric propagation factor. Semi-empirical models interconnect the three ionospheric peak parameters analyzed here and as such their individual variations and comparison with global empirical model such as IRI must not be assumed. There exists also an obvious gap in that thorough quantitative comparison analysis between model and measurement of ionospheric parameters are limited.

The overall model error, that is the mean square root deviation of the model from the data over the representative month ranging from about 6–8% (h_mF_2), ∼13–38% (f_oF_2) and ∼8–29% (h_mF_2), ∼12–44% (f_oF_2), respectively for low and high flux year, but approximately comparable at ∼3–7% for $M_{3000}F_2$ during solar minimum and maximum conditions. Accordingly, the largest error is clearly seen in f_oF_2 and smallest in h_mF_2, while error in $M_{3000}F_2$ is not evident. The CCIR model reproduced well the propagation factor. The CCIR $M_{3000}F_2$ model uses a low order of spherical harmonics and therefore cannot reproduce the sunrise and sunset peaks (D. Bilitza, personal communication, 2011).

There exist noticeable seasonal differences between the data and the model results. The largest percent disparity occurs in f_oF_2 (URSI: 3–80%, CCIR: 7–66%), lowest in $M_{3000}F_2$ (0–14%), and medium value in h_mF_2 (0–19%) during low solar activity year. During solar maximum year, the seasonal variation is also prominent in f_oF_2 with percent difference, 0–82% (URSI) and 3–70% (CCIR), the smallest in $M_{3000}F_2$, 0–12%. The percent discrepancy noted in h_mF_2 is 0–22%. We immediately observe that solar activity seems to play less significant role in percent deviations. The sharp post-midnight increase in h_mF_2 during low solar activity in July 1987 at 0200 LT (see observation 1) correspond to a deep minimum in $M_{3000}F_2$ at the same time and month (see observation 5), sunrise minimum noted in h_mF_2 during high solar activity of July 1990 also corresponds to a sharp increase in $M_{3000}F_2$ at the same time and season of high solar flux year (see observation 6) confirm the strong anti-correlation that exists between h_mF_2 and $M_{3000}F_2$.

It is hypothesized that the F_2-layer in low magnetic latitudes is strongly influenced by electric fields, the "fountain effect" described by Hanson and Moffett (1966) and many others. The vertical drift is upward by day and downward by night. This upward daytime flow, combined with poleward meridional transport and eventual downward diffusion, leads to a redistribution of plasma referred to as the "fountain effect". Consequently, we expect to see strong signature of this behavior in the key equatorial ionospheric F_2-layer parameters. Also due partly to the day-to-day variability of the detailed electrodynamics and dynamics processes in the equatorial ionosphere; both f_oF_2 and h_mF_2 have peculiarities in the equatorial region, magnetic hemispheric and longitudinal behaviors. Thus, these complex processes that influenced ionospheric characteristics over equatorial region provide unique challenges for empirical modeling of the region. Another reason for remarkable differences between model and observational results is that the data coverage in the IRI model is limited to certain geographical locations and there is scarceness of ionospheric data at other locations, especially in global equatorial zones. A further complication arises owing to our limited understanding of the interplay between production, recombination, dynamics and electrodynamics processes in the equatorial F_2-layer. However, F_2-layer is presumably connected in some ways with the magnetospheric processes from above and processes from lower atmosphere, in this way, the upper ionosphere is intricate to predict.

5. Summary

In this research, we have analyzed ionosonde measurements recorded at a near equatorial station, Ouagadougou in order to validate ionosonde F_2-layer parameters against the global empirical International Reference Ionosphere (IRI-2007; Bilitza and Reinisch, 2008) at the low and high levels of solar activity and magnetically quiet conditions for four distinct seasonal periods in the equatorial F-region in the West-African sector. The major highlights of our investigation are delineated as follows:

1. Generally, IRI-predicted model portrays convincingly well the salient features and phenomena of equatorial

ionosphere. Although the simulation results overpredicts h_mF_2 values over Ouagadougou in all seasons at the two levels of solar activity, especially during the daytime, but the nighttime value is reasonably reproduced. On the other hand, the model seriously underpredicts f_oF_2 in all seasons for the two solar activity conditions, except for January and October 1987 and URSI option in January 1990.

2. The magnitudes of the calculated differences for both low and high solar flux periods essentially exhibit significant percent deviations, particularly for h_mF_2 and f_oF_2. Comparisons of the hourly percent deviation of f_oF_2 with comparative analysis recently reported by Oyekola (2011) for Ibadan, Nigeria (7.4°N, 3.9°E; dip latitude: 2.3°S) within West African longitude sector show marked longitude differences at equatorial zone. These must be due to some longitude-dependent factor, most probably connected in several ways with the detailed electrodynamics and dynamics of equatorial ionosphere. The highlighted longitude and magnetic hemispheric disparities between Ibadan and Ouagadougou will be valuable for the improvement of the predictability of IRI model in one hand, and update of IRI model on the other hand, for equatorial region.
3. Our results show good reasonable agreement between the IRI predictions and the $M_{3000}F_2$ measurements for all seasons at low and high sunspot periods. Although dawn maximum and post-sunset minimum clearly seen in observational $M_{3000}F_2$ data are not followed by the model.
4. This analysis provides further important clues towards a better understanding of the occurrence of post-midnight equatorial F-region irregularities (EFIs), which are known to develop mainly during solar minimum June solstice periods over African longitude sector (Li *et al.*, 2011). Thus, this work confirms the dominant role of day-to-day variability in the electrodynamic processes in causing large deviations of the measured f_oF_2 and estimated h_mF_2 from the modeled results.
5. Our observations present higher values of f_oF_2 deviations from the model compared to the earlier results obtained for the low-latitude longitude sectors over Indian and Southeast Asian quoted in this paper.
6. Lastly, the study sum up the appreciable success of the IRI simulations in explaining prominent observed characteristic diurnal and seasonal features and other phenomena of equatorial ionosphere.

Acknowledgments. We thank the referees for their helpful remarks and suggestions, particularly pointing out scientific and technical and language observations in the paper. Of course, the great job they have done together with insightful comments of Dr. Dieter Bilitza (guest editor) on the original draft of this paper made this work the way it appears now. We gratefully acknowledge United State National Oceanic and Atmospheric Administration (NOAA) for providing h_mF_2, f_oF_2, and $M_{3000}F_2$ data from the IRI2007 model website.

References

Abdu, M. A., I. S. Batista, B. W. Reinisch, J. H. A. Sobral, and A. J. Carrasco, Equatorial F region evening vertical drift, and peak height, during southern winter months: A comparison of observational data with the IRI descriptions, *Adv. Space Res.*, **37**, 1007–1017, 2006.

Adeniyi, J. O., D. Bilitza, S. M. Radicella, and A. A. Willoughby, Equatorial F2-peak parameters in the IRI model, *Adv. Space Res.*, **31**(3), 507–512, 2003.

Araujo-Pradere, E. A., T. J. Fuller-Rowell, and D. Bilitza, Ionospheric variability for quiet and disturbed conditions, *Adv. Space Res.*, **34**, 1914–1921, 2004.

Batista, I. S. and M. A. Abdu, Ionospheric variability at Brazilian low and equatorial latitudes: comparison between observations and IRI model, *Adv. Space Res.*, **34**, 1894–1900, 2004.

Bertoni, F., Y. Sahai, W. L. C. Lima, P. R. Fagundes, V. G. Pillat, F. Becker-Guedes, and J. R. Abalde, IRI-2001 model predictions compared with ionospheric data observed at Brazilian low latitude stations, *Ann. Geophys.*, **24**, 2191–2200, 2006.

Bilitza, D., International reference ionosphere 2000, *Radio Sci.*, **36**(2), 261–275, 2001.

Bilitza, D., International reference ionosphere 2000: Examples of improvements and new features, *Adv. Space Res.*, **31**(3), 757–767, 2003.

Bilitza, D. and B. W. Reinisch, International reference ionosphere 2007: Improvements and new parameters, *Adv. Space Res.*, **42**(4), 599–609, doi:10.1016/j.asr.2007.07.048, 2008.

Bilitza, D., N. M. Sheikh, and R. Eyfrig, A global model for the height of the F2-peak using M3000 values from the CCIR numerical maps, *Telecomun. J.*, **46**(9), 549–553, 1979.

Bilitza, D., C. Koblinsky, B. Beckley, S. Zia, and R. Williamson, Using IRI for the computation of ionospheric corrections for altimeter data analysis, *Adv. Space Res.*, **15**(2), 113–120, 1995.

Bradley, P. A. and J. R. Dudeney, A simple model of the vertical distribution of electron concentration in the ionosphere, *J. Atmos. Sol.-Terr. Phys.*, **35**, 2131–2146, 1973.

Chuo, Y. J. and C. C. Lee, Ionospheric variability at Taiwan low latitude station: Comparison between observations and IRI-2001 model, *Adv. Space Res.*, **42**, 673–681, 2008.

Coetzee, P. J., Applications of the IRI in South Africa, *Adv. Space Res.*, **34**, 2075–2079, 2004.

Hanson, W. B. and R. J. Moffett, Ionization transport effects in the equatorial F-region, *J. Geophys. Res.*, **71**, 5559–5572, 1966.

Huang, C., C. Liu, H. Yeh, W. Tsai, C. Wang, K. Yeh, K. Lin, and H. Tsai, IRI model application in low latitude ionospheric topography, *Adv. Space Res.*, **18**(6), 237–240, 1996.

Lee, C.-C. and B. W. Reinisch, Quiet-condition hmF2, NmF2, and Bo variations at Jicamarca and comparison with IRI-2001 during solar maximum, *J. Atmos. Sol.-Terr. Phys.*, **68**, 2138–2146, 2006.

Li, G., B. Ning, M. A. Abdu, X. Yue, L. Liu, W. Wan, and L. Hu, On the occurrence of postmidnight equatorial F region irregularities during the June solstice, *J. Geophys. Res.*, **116**, A04318, doi:10.1029/2010JA016056, 2011.

Miller, K., A. Hedin, P. Wilkinson, D. Torr, and P. Richards, Neutral winds derived from IRI parameters and from the HWM87 wind model for the Sundial campaign of September 1986, *Adv. Space Res.*, **10**(8), 99–102, 1990.

Obrou, O. K., D. Bilitza, J. O. Adeniyi, and S. M. Radicella, Equatorial F2-layer peak height and correlation with vertical ion drift and M(3000)F2, *Adv. Space Res.*, **31**(3), 513–520, 2003.

Oyekola, O. S., Variation in the ionospheric propagating factor M(3000)F2 at Ouagadougou, Burkina Faso, *Adv. Space Res.*, **46**(1), 74–80, 2010.

Oyekola, O. S., Comparisons of foF2 with IRI model and equatorial vertical drifts, *Adv. Space Res.*, **48**(8), 1318–1326, doi:10.1016/j.asr.2011.06.027, 2011.

Pawlowski, D. J., A. J. Ridley, I. Kim, and D. S. Bernstein, Global model comparison with Millstone Hill during September 2005, *J. Geophys. Res.*, **113**, A01312, doi:1029/2007JA012390, 2008.

Rios, V. H., C. F. Medina, and P. Alvarez, Comparison between IRI predictions and digisonde measurements at Tucuman, *J. Atmos. Sol.-Terr. Phys.*, **69**, 569–577, 2007.

Sethi, N. K., R. S. Dabas, and K. Sharma, Comparison between IRI predictions and digital ionosonde measurements of hmF2 at New Delhi during low and moderate solar activity, *J. Atmos. Sol.-Terr. Phys.*, **70**, 756–763, 2008.

Sobral, J. H. A., M. A. Abdu, P. Muralikrishna, J. Labelle, V. M. Castilho, and C. J. Zamlutti, Rocket and ground-based electron density soundings

versus IRI representation, *Adv. Space Res*., **31**, 569–575, 2003.

Wilkinson, P. J., Ionospheric variability and the international reference ionosphere, *Adv. Space Res*., **34**, 1853–1859, 2004.

Yadav, S., R. S. Dabas, R. M. Das, A. K. Upadhayaya, K. Sharma, and A. K. Gwal, Diurnal and seasonal variation of F2-layer ionospheric parameters at equatorial ionization anomaly crest region and their comparison with IRI-2001, *Adv. Space Res*., **45**, 361–367, 2010.

Zhang, M. L., J. K. Shi, X. Wang, and S. M. Radicella, Ionospheric variability at low latitude station: Hainan, China, *Adv. Space Res*., **34**, 1860–1868, 2004a.

Zhang, M. L., J. K. Shi, X. Wang, S. Z. Wu, and S. R. Zhang, Comparative study of ionospheric characteristic parameters obtained by DPS-4 digisonde with IRI2000 for low latitude station in China, *Adv. Space Res*., **33**, 869–873, 2004b.

O. S. Oyekola (e-mail: oyedemio@yahoo.com) and P. R. Fagundes